energies

MDPI

Article

Real-Time Detection of Karstification Hazards While Drilling in Carbonates †

Danil Maksimov *, Alexey Pavlov and Sigbjørn Sangesland

Department of Geoscience and Petroleum, NTNU Norwegian University of Science and Technology, S.P. Andersens vei 15a, NO-7491 Trondheim, Norway; alexey.pavlov@ntnu.no (A.P.); sigbjorn.sangesland@ntnu.no (S.S.)

* Correspondence: danil.maksimov@akerbp.com

† This paper is an extension of a conference paper. In Proceedings of the International Conference on Offshore Mechanics and Arctic Engineering, Online, 3–7 August 2020.

Abstract: The nature of carbonate deposition can cause the development of unique geological features such as cavities and vugs called karsts. Encountering karsts while drilling can lead to serious consequences. To improve drilling safety in intervals of karstification, it is important to detect karsts as early as possible. The use of state-of-the-art geophysical methods cannot guarantee early or even real-time detection of karsts or karstification zones. In this paper we demonstrate, based on an analysis of 20 wells drilled in karstified carbonates in the Barents Sea, that a karst that is dangerous for drilling is often surrounded by one or more other karstification objects, thus forming a karstification zone. These zones can be detected in real time through certain patterns in drillstring mechanics and mud flow measurements. They can serve as indicators of intervals with a high likelihood of encountering karsts. The identified patterns corresponding to various karstification objects are summarized in a table and can be used by drilling engineers. Apart from that, these patterns can also be utilized for training machine learning algorithms for the automatic detection of karstification zones.

Keywords: carbonate; karst; geophysics; hazards mapping; karst prediction

Citation: Maksimov, D.; Pavlov, A.; Sangesland, S. Real-Time Detection of Karstification Hazards While Drilling in Carbonates. *Energies* **2022**, *15*, 4951. https://doi.org/10.3390/en15144951

Academic Editors: Yongwang Liu, Kanhua Su and Yuanxiu Sun

Received: 6 May 2022
Accepted: 25 June 2022
Published: 6 July 2022

1. Introduction

Carbonate reservoirs produce a significant volume of the world's total oil and gas [1]. Many of the world's carbonate reservoirs have considerable potential for development and production. However, the history of drilling has shown that the heterogeneous nature and the complexity of the rock properties of carbonate reservoirs make them challenging to drill. Karstification processes often affect carbonate reservoirs and cause the development of a number of unique geological features called karsts. Here we refer to a common definition of the karst, introduced to describe the landscape, which contains caves, underground channels, and other features associated with soluble rocks [2]. Encountering karsts while drilling can cause critical safety incidents including uncontrollable losses of drilling fluid and gas kicks as reported in speciality reports [3–6].

There are several ways to mitigate these risks. The volume of mud loss in some conductive fractures can be successfully controlled by varying the concentration of Loss Circulation Materials (LCM) or by changing the chemical composition of the mud [7,8]. Usually, these measures have only a short-term effect and require more and more chemicals and cement materials leading to additional costs and delays [9].

The most common solution to mitigate many of the problematic situations encountered in karstified carbonates is the use of Managed Pressure Drilling (MPD) and its modifications, such as Pressurized Mud Cup Drilling (PMCD). In PMCD, a sacrificial fluid is pumped through the bit nozzles to fill any fractures and caves, while a heavier fluid is pumped into

the annulus to maintain the mud cap and prevent gas migration up to the surface. Today this is the most common practice for drilling in carbonates used by drilling companies [10–14].

However, for PMCD there is an operational necessity for additional equipment installation on the rig site such as the Rotational Controlled Device (RCD) [15]. Additionally, a significant volume of sacrificial fluid is required for drilling, which makes this technique inapplicable in some regions. In the case of exploration drilling, the rig may not be equipped for PMCD before drilling begins due to underestimation of drilling risks. PMCD does not solve all karst-related challenges. An excessive shock can act on the drill bit when the Bottom Hole Assembly (BHA) suddenly reaches the bottom of a cave. It can break the drillstring with possible lost in hole and stuck-pipe events. To avoid such scenarios, it is necessary to predict or detect individual karsts and/or zones with a high likelihood of karsts and, based on this information, act to minimize the possibility and potential consequences of drilling into a karst.

Another solution is based on prediction, detection and avoiding drilling into karstification objects, which is developing technologies to investigate subsurface structures. Today we benefit from cutting-edge methods within geophysical research. However even with the most advanced geophysical methods it is still challenging to detect karsts and avoid drilling into them.

The standard seismic-based techniques for mapping reservoirs, faults, and structural surfaces can be effective for the detection of *large* karst structures [16,17]. However, not all karsts can be detected by seismic intervention. Along with the successful case studies, the main limitation in the seismic detection of karsts is related to the problem of vertical resolution [18]. It has been shown that caves less than $\frac{\lambda}{4}$ (40 m (131 ft)) cannot be separated due to wave interference [19]. In certain regions in the Barents Sea, encountered caves were less than a meter and they were very dangerous for drilling [20].

A wide range of investigative logging while drilling measurements (LWD) can be used to detect karsts. For example, borehole acoustic reflected survey (BARS) [21], and ultradeep resistivity tools [22] are among the most promising. Although effective in certain cases [23,24], the main drawback of LWD tools is that the vast majority of them provide look-around measurements (also usually at a great distance from the bit) and do not look ahead of the bit. Thus, the area ahead of the bit cannot be investigated by direct measurements. Any relevant measurements from LWD tools come with a significant delay (due to the large offset from the drill bit) and are, therefore, not suitable for real-time decision making on mitigating karst-related risks.

It is challenging with current technologies to detect individual karsts ahead of the bit and real-time decision making and risk mitigation needs an approach that can provide real-time identification of areas with a high likelihood of encountering karsts. Detection of such karstification zones can be vital for real-time decision making and minimization of drilling risks in karstified carbonates. This approach requires answering the following questions: (1) Are there karstification objects around karsts that are dangerous for drilling that can be detected and used to identify that karstification zone? (2) Can these karstification objects be detected in real time from drilling measurements and what measurement patterns correspond to them? These patterns can then serve as indicators of karstification zones.

In this paper we take this last approach and address the above questions based on an in-depth analysis of drilling data from 20 wells drilled in karstified carbonates in the Barents Sea. The method of karst patterns detection based on real-time drilling measurements described in this manuscript is limited in terms of the number of wells available for the analysis. Even in closely-studied fields, the percentage of wells, which encountered karsts and at the same time contained a full set of necessary well-log data, as will be discussed in the following sections, is rather small. Being limited to a specific area of the Loppa High Region, the study presented in this paper does not include other geographical regions of karstification. However the presented methodology can be utilized regardless of the geography of the research region. This will allow the creation of a more complete and

statistically reliable picture of real-time indicators of karsts and karstification zones to be used for safer drilling in karstified carbonates.

1.1. Karstification Objects

To answer these research questions, it is important to understand the nature and genesis of karsts. There are a number of processes contributing to karstification. Dissolution of soluble rocks by meteoric waters along pathways specified by a geological structure is considered one of the main mechanisms of karstification [25]. However, by itself the solubility of the rock is not sufficient to form a karst. Favorable geology, formation lithology, rock mechanical properties, burial depth of carbonates, rock fracturing and other characteristics are important factors for karst development. Karsts and signs of karstification can be found at different depths and can be observed as various large and small-scale surface or subsurface objects. The most remarkable feature of subsurface karsts is the cave. Erosion by chemicals and turbulent streams are often factors affecting the development of underground corrosion and fluvial caves [26]. Some of the caves can be connected into network of channels (anastomotic caves), while others are isolated caves called voids and range from the vug-sized small scale, up to the full cave scale.

The size of caves is limited and as soon as a certain limit is reached, the cave starts to collapse [27]. Products of collapse—called cave-collapse breccia—are composed of different angular fragments with the interspace filled by finer sediments or matrix particles [28].

Sometimes it is mistakenly assumed that open (not collapsed) cave systems occur only at shallow depths. However there are examples of caves buried at 6000–8000 m (19,685–26,246 ft) depth with the average vertical size varying from 100 to 300 m (328–984 ft) [29]. Karstification is a complex process and the results of this process can be everything from small-scale porosity up to large cave systems. While porosity plays an important role for reservoir development, karstification objects pose significant challenges for drilling due to the high risks associated when crossing a system of caves or vugs. Drilling into a cave or a systems of caves/vugs can have serious consequences for drilling including lost circulation of drilling fluid and gas kicks.

For example, Shell reported that total losses were observed in each of the six wells when drilling in carbonates in Sarawak (Peninsular Malaysia) [30]. Similar problems exist on the Norwegian Continental Shelf when drilling into open fractures or karsts resulted in total losses during a week [20,31,32]. Two to four weeks of non-productive time were reported by an operator company in Qatar when a large volume of cement was pumped to plug intervals of mud losses in carbonates [33]. In the worst case scenario, total mud losses can lead to gas kicks of different severity due to underbalanced downhole conditions.

There are other known challenges associated with drilling in carbonates. Poor hole cleaning, high shock and vibrations in the Bottom Hole Assembly (BHA) and lower Rate Of Penetration (ROP) than in other formations [34]. These issues have fewer consequences for safety and rarely lead to losing control over the well. Moreover, some of them can be successfully mitigated within current drilling practices in carbonates by optimizing the drilling parameters or by changing configurations of the BHA [35,36].

1.2. Contribution

The lack of available technologies to predict and prevent drilling into a karst that is dangerous for drilling motivates our study. Our working hypothesis is the following. Geological conditions that lead to forming a karst that is dangerous for drilling extend over some distance around the karst and lead to the development of other karstification objects in that area. These karstification objects may not be dangerous for drilling. Yet, they can serve as indicators of drilling through an interval with geological conditions favorable to the development of karsts and, thus, with a high likelihood of encountering karsts that are dangerous for drilling. Early detection of such intervals can be used for risk mitigating actions such as rigging up Managed Pressure Equipment (MPD), Lost Circulation Materials (LCM) rig-logistics, optimization of well path and well geological targets.

Both major and minor karstification objects may be detectable from real-time drilling data. A minor mud loss, for example, may correspond to drilling into such a karstification object. If one can find patterns in real-time drilling measurements corresponding to karstification objects, these patterns can be used for the detection of karstification intervals.

In this paper, we support the presented hypothesis with in-depth analysis of 20 wells drilled in carbonates in the Loppa High region in the Barents Sea. The analyzed data correspond to a very rare combination of drilling through karstified carbonates with logged borehole images and accurate mud flow-rate measurements. This combination enables the detailed analysis presented in this paper.

Based on this analysis, we demonstrate that there are intervals with karstification objects around karsts that are dangerous for drilling. Minor karstification objects contained in these intervals can be detected from real-time drilling data and serve as indicators for higher likelihood of encountering karsts that are dangerous for drilling. We identify and present patterns in real-time drilling data corresponding to various karstification objects. These patterns can either be used for manual detection of karstification objects (and intervals) or they can be employed by advanced analytics tools, such as machine learning, for the automatic detection of karstification objects (and intervals) from real-time drilling data.

To the best of the authors' knowledge, no such analysis has been reported in the literature on drilling in karstsified formations so far. In fact, the percentage of wells encountering karsts and, at the same time, containing necessary well-log data (e.g., borehole images) is rather small. This leads to a general lack of in-depth studies of karst phenomena in drilling. This paper attempts to fill in this gap and also presents a methodology that can be utilized in further studies of karsts in drilling.

1.3. Methodology

We started the analysis with a detailed study of drilling events and end-of-well reports. Based on this analysis we obtained an overview of rig-site drilling events for all wells within the region of study. Joint analysis of the rig-site events confirmed the existence of karstification intervals with specific BHA behavior such as reported drilling breaks, high levels of shocks, and mud losses. The conclusion that there are karstification objects/zones around karsts that are dangerous for drilling was also confirmed by a number of specific examples analyzed with borehole images and core samples. Second, we performed localization of karstification objects along the well-paths based on borehole image data. This provides a better understanding of the karstification problem in the Loppa High region and karstification phenomena in general and serves the next step. Third, we correlated the logged drilling data with the localized karstification objects. We conducted a detailed analysis of the corresponding time-domain data of BHA dynamics and mud flow data and summarized identified patterns corresponding to various karstification objects in a table.

1.4. Paper Organization

In Section 2, we review drilling experience in karstified carbonates in the Barents Sea and describe the mapping of karstification objects along the wellbore from the logged borehole image data. Section 3 studies the drilling mechanics in the mapped karstification intervals to identify specific patterns in real-time measurements corresponding to karstification objects. In Section 4 we investigate mud flow measurements to identify additional flow-based indicators of karsts. Conclusions, discussion and suggestions for future work are presented in Section 5.

2. Karsts Mapping—Borehole Images and Drilling Events Study

2.1. Region of Study

The studied area is located in the Barents Sea and is the largest of the three defined offshore petroleum provinces in Norway: the North Sea, the Norwegian Sea and the Barents

Sea. The study will focus on the recent discoveries in the Loppa High region—Alta and Gohta, as shown in Figure 1. They are located 160 km (100 miles) off the coastline with a water depth 300–400 m (980–1300 ft).

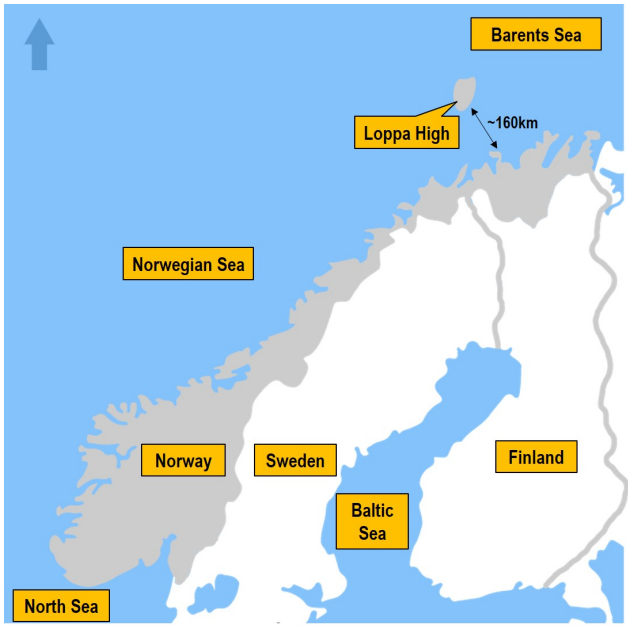

Figure 1. Barents Sea, Loppa High Region, Alta and Gohta Discoveries.

The seafloor in the studied region consists of complex patterns, formed as a result of considerable uplift and Cenozoic era erosion. Uplift has brought high density rocks close to the seafloor. This creates additional difficulties for seismic studies of the region [37]. This tectonic event led to the development of a complex underlying structure with an extensive faulting and significant altitude change of more than 1000 m (3281 ft) (Kobbe formation).

Deeper layers of naturally fractured carbonates were weathered and buried. This caused karstification with a subsequent development of voids. Some of the larger karsts and voids are collapsed and filled with sediments, others remain "open". These regional features have become a significant challenge for drilling.

2.2. Drilling Data Analysis

We consider drilling data from 20 wells drilled in karstified carbonates. These wells characterized by an extended set of data available for analysis, including drilling data (mud logs, drilling reports, site survey reports), drilling mechanics data (surface and downhole measurements), geology (lithology, stratigraphy, biostratigraphy), rock and core (conventional core analysis and core photos), petrophysical reports (CPI, Composite), well logs (wireline, LWD).

Once all the available data were analyzed, we obtained an overview of the entire field. Part of this analysis is displayed in Figure 2. Joint analysis of these data is revealing in several ways. First, the events attributed to karstification objects occur in intervals containing minor and/or major events. When identified, these events can serve as indicators of karstification intervals. In a number of cases drilling breaks and tight spots are encountered close to cave or breccia intervals. This determines the need for a detailed study of drillstring mechanics measurements as a potential means to detect karstification objects in real time. The results of this analysis will be discussed in Section 3. Second, drilling in breccia intervals is often accompanied by mud losses of varying volumes. In Section 4 we will examine mud flow data as another means to detect karstification objects.

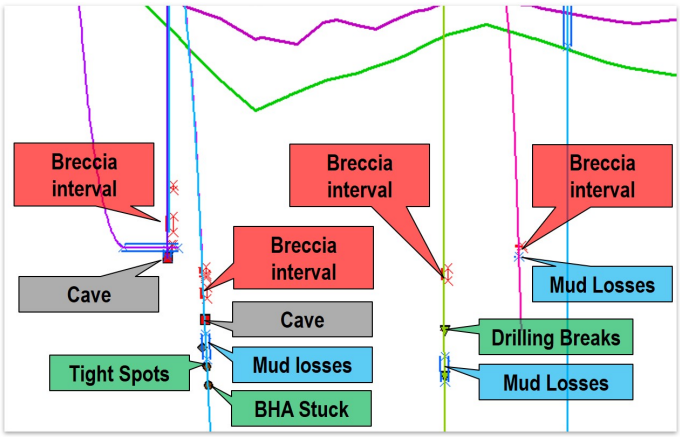

Figure 2. Drilling events in the karstification intervals.

2.3. Mapping of Karstification Objects

To study drillstring mechanics and mud flow effects corresponding to karstification objects, we needed to localize these objects along the wellbores. This localization was performed based on borehole images. Borehole imaging is commonly used in the oil and gas industry. The interpretation of image data is intended to determine the magnitudes, azimuths and geometrical properties of numerous geological features along the wellbore. The image tools can provide images of vugs, breccias, caves and other karst forms. Image of the wellbore is the "unrolling" of a wellbore picture along the well path. Physical principles underlying borehole imaging tools are the propagation of ultrasonic waves and electrical conductivity of the formation. Below we present some examples of karstification objects identified in the analysis of borehole images.

Two examples of subsurface karstification objects—collapsed breccias—identified along a borehole are presented in Figure 3. Patchy patterns of the low resistive black surrounding the light brown resistive pattern could be interpreted as breccia. The breccias in this example are considered to be formed due to the collapse of a cavity that was possibly created by evaporate dissolution. These two breccia intervals were identified by borehole geologists. This collapsed cavity was successfully drilled through without any drilling challenges. However, the detection of this type of karst form may serve as an indicator of a karstification interval with increased likelihood of encountering other karst forms that can pose significant risks to drilling.

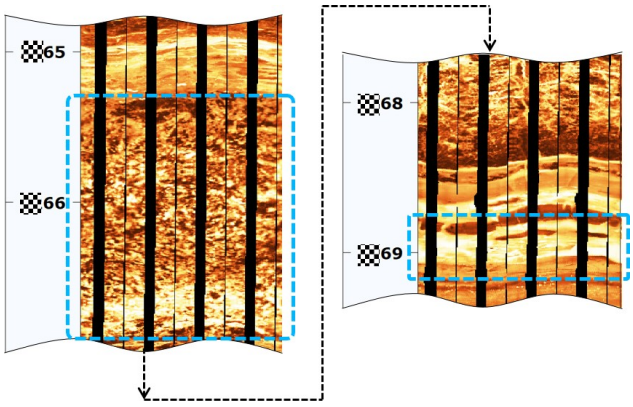

Figure 3. Example of breccias developed due to cavity collapse.

In another example, shown in Figure 4, the well path crossed an interval of conductive vugs up to dm scale size and then intersected a cavern, which is open to the fluid flow. Geometrical properties of the cavern are not defined. However, the part, which can be seen in the borehole image is more than 50 cm (19.7″) in length with circumference of 21.6 cm

(8.5″ section of the well). This case demonstrates the geological signs preceding the later encountered cave. As can be noted from the image data, the first signs of karstification appeared more than 10 m ahead of the cave. Potential detection of these signs, based on drilling data and in real time, can contribute to decision support while drilling.

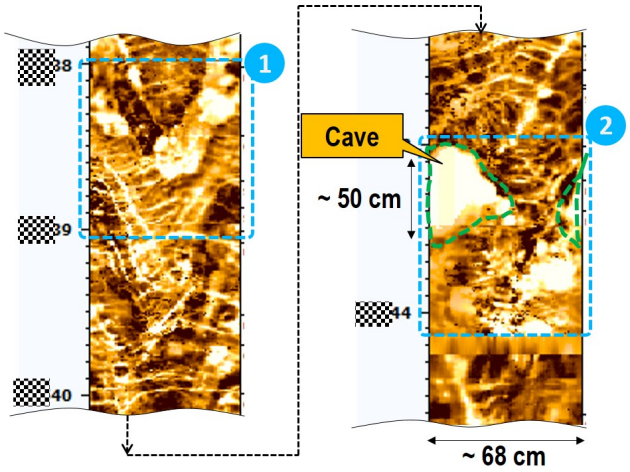

Figure 4. Example of vugs preceding a cave.

These two examples correspond to over 12 karstification objects identified from the borehole images and studied in this analysis. The overall results indicate that karstification objects and the corresponding drilling events, minor or major, are often encountered in sequences corresponding to karstification intervals rather than individual objects. Vugs and breccia forms can be considered indicators of karstification intervals. In several cases they preceded drilling into a larger cave. These are not karstification objects that we describe in this section.

Borehole imaging is a very powerful tool in terms of the identification of a variety of geological attributes. However, it is unsuitable for real-time detection of karst forms and karstification intervals. Typical sources of borehole images are Wire Line (WL), which is recorded after a certain interval or section of the well has been drilled, and LWD tools, which have significant sensor-bit offset and a data-transmission/processing delay and, thus, cannot provide real-time data. This demonstrates the necessity to determine a set of real-time measurements that can reveal signs of karstification while drilling. An analysis of such measurements is presented in the two following sections.

3. Detection of Karsts Based on Drilling Mechanics

In this section, we consider a set of real-time drilling measurements, which can demonstrate specific responses in the intervals of karsts. This set of measurements may be used as the first set of indicators for real-time detection of zones with a high likelihood of encountering karsts. Although in this section we will focus primarily on the drillstring dynamics, hydraulic data will also be considered as an auxiliary factor for better understanding drilling events.

Let us first briefly discuss the measurements that will be studied in this section. Among the surface measurements considered in this analysis we will focus on (1) Rate Of Penetration (ROP)—distance drilled per time, derived from the block position measurement, and (2) Hookload—the weight on the hook to control the weight applied on the bit (WOB). Hydraulic measurements, which will be studied in more detail in the next section, but also mentioned here, include mud flow rates in and out of the wellbore. Their difference, called delta-flow indicates mud gains or losses in the wellbore. Accumulated, they lead to changes in the fluid volume in the mud tank. For more information on how these measurements can be used we refer readers to speciality reports [38–40].

The downhole set of measurements provide an opportunity to study the efficiency of transferring surface energy downhole. Introduced in the 1980s, they are a vital source of information about drillstring behavior [41–43]. These sensors are mounted on the drillcollar close to the drill bit. A horizontal strain-gauge measures torque acting on the drill bit, while a vertical strain-gauge can measure the bit on- off-bottom weights. Since these gauges are located very close to the drill bit, we utilize them to evaluate possible changes in drilling dynamics in the intervals of karststification. Along with the downhole WOB and torque measurements, a three-axis accelerometer is typically incorporated into the downhole acquisition sub, in order to measure changes of the acceleration magnitudes in axial, tangential and radial directions of the BHA [44].

Drilling measurements, either surface or downhole, are affected by changes in the downhole conditions (e.g., formation properties) and in operational parameters specified by the driller. Since we are interested in formation properties, we study only time intervals where the operational parameters specified by the driller remain constant. This helps to eliminate changes in drilling measurements, which are not related to geological signs of karstification.

Drilling in carbonate reservoirs is frequently accompanied by a high level of Shocks and Vibrations (S&V). This measurement will be the first drilling mechanics measurement we focus on when identifying responses to drilling through karstification objects. Another measurement we focus on is ROP in the intervals of karstification.

Typically, there are a number of drilling parameters, which have considerable influence on the ROP. This influence is far from simple and its analysis lies outside the scope of this paper. However, ROP is an essential parameter for karst detection as it is directly linked to rock properties. This principle underlies many studies devoted to drillability, which was first defined by Teale [45] as the ability of a rock to be drilled. Overall, Teale's study [45] highlights that the rock properties such as Uniaxial Compressive Strength (UCS), brittleness, abrasiveness, texture, mineralization and many other, also influence ROP apart from drilling parameters [46]. An implication of these facts is that for constant drilling parameters, fluctuations of the ROP while drilling are most probably be related to rock properties. For early karst detection, as will be illustrated later, ROP variations might be an indicator of drilling through different karstification objects such as breccias, vugs or caves. Even though variations in ROP and S&V are closely related to rock properties, one often needs to consider the whole picture, including other measurements to detect karstification objects from the measurements.

Below we present a number of examples demonstrating the effects of karstification objects on drilling mechanics measurements. These examples also support the conclusion of Section 2 that there are various signs of karstification around karsts that in certain cases can be detected through real-time measurements.

We start with an example of drilling in the Ørn Formation (Well #1). This formation is dominated by marine, shelf/platform carbonates with bryozoan bioherm build ups and shallow marine, supra-tidal carbonates. Initial analysis of drilling events in Well #1 reveals the following cases. During the core-sampling run, the BHA dropped 2 m without WOB. The initial loss rate was 40 m^3/h (176.1 gal (US)/min) and escalated to the total mud loss situation. A full well control incident came into effect. This sequence of events demonstrates the result of drilling into an open cave. However, the most important research information here are the signs of karstification in the interval above the discovered cave. As this cave was discovered during coring of Well #1, there is rather limited information for drilling mechanics analysis, for example, there is no information about S&V and there is no borehole image data available for this interval. So we have to rely on other sources of information: drilling fluid measurements and core samples.

A number of small mud losses were observed in the interval Well #1 more than 10 m (32.8 ft) above the cave. This allows us to assume the possible presence of a conductive system of vugs and/or the presence of a breccia zone, as mentioned earlier.

This assumption is confirmed by the core-sample photos, which were acquired after Core Run 1. As shown in Figure 5, the interval of 20 m (65.6 ft) above the cave is presented by brecciated dolomites, cemented clasts of different size and shape. In the interval 15 m (49.2 ft) above the cave, it can be noticed cm-scale round to oval conductive spots, which may be interpreted as vugs, probably formed due to dissolution of the massive facies by corrosive fluids. The core sample closest to the cave is 10 m (32.8 ft) above the cave and has weekly cemented carbonate.

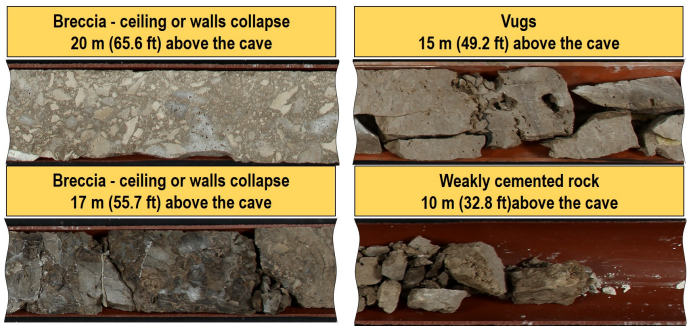

Figure 5. Core-samples photos of the interval preceding the cave (Well #1)

Surface and downhole drilling measurements versus time are shown in Figure 6. This is a common representation of drilling data to analyze the performance of the BHA or study the drilling process.

In this example we notice recurring mud loss events at a distance of 6 and 5 m from the cave marked with arrow number 1 in Figure 6. These intervals correlate with fluctuations of WOB, a small decrease in the first mud loss interval and a considerable decrease in the second interval of mud losses. Since the rest of drilling parameters remain the same when the WOB changed, this might be a sign of drilling through intervals with different mechanical properties. Before the cave interval, there are a number of sharp ROP increases, with simultaneous growing of the hook load (arrow #3) and WOB decrease (arrow #4), which can be interpreted as drill breaks pointed out by arrow #5 in the figure, caused by drilling through karstification objects.

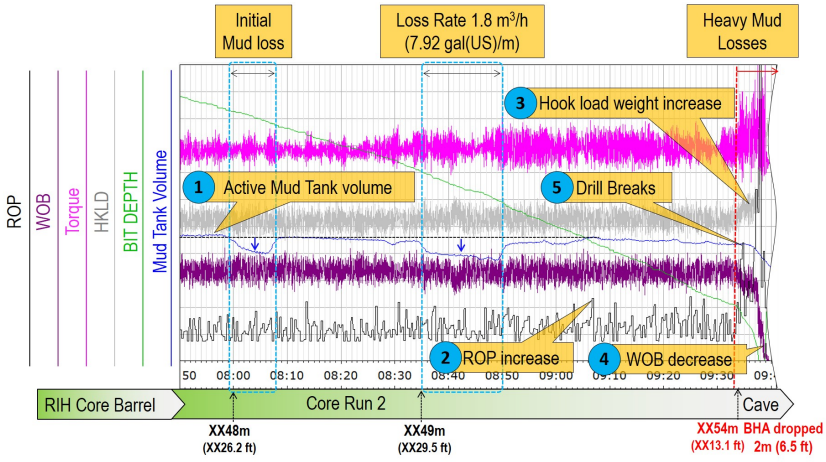

Figure 6. Drilling mechanics data in the interval close to cave (Well #1).

The next example demonstrates the drilling of Well #2 through an interval of conductive patches, which are interpreted as large vugs, probably formed due to post-depositional (e.g., karstic) carbonate dissolution. The interval is identified based on borehole imaging, where dark areas in the acoustic image represent low-amplitude response (Figure 7). This interval is interpreted as carbonate with large vugs facies, dm-scale, conductive, irregular features. As can be seen in Figure 7, there is a rapid increase in the S&V in the interval of

vugs, marked with the arrow #1. The drilling regime remains constant within this interval, as can be seen by the constant value of the hookload. However we can clearly see the high torque (arrow #2) and ROP (arrow #3), which enables us to conclude that these changes of S&V might be related to the vugs facies. As in the previous case this case also demonstrates an increase in ROP, which might be explained by faster drilling through small cavities inside the rock (vugs).

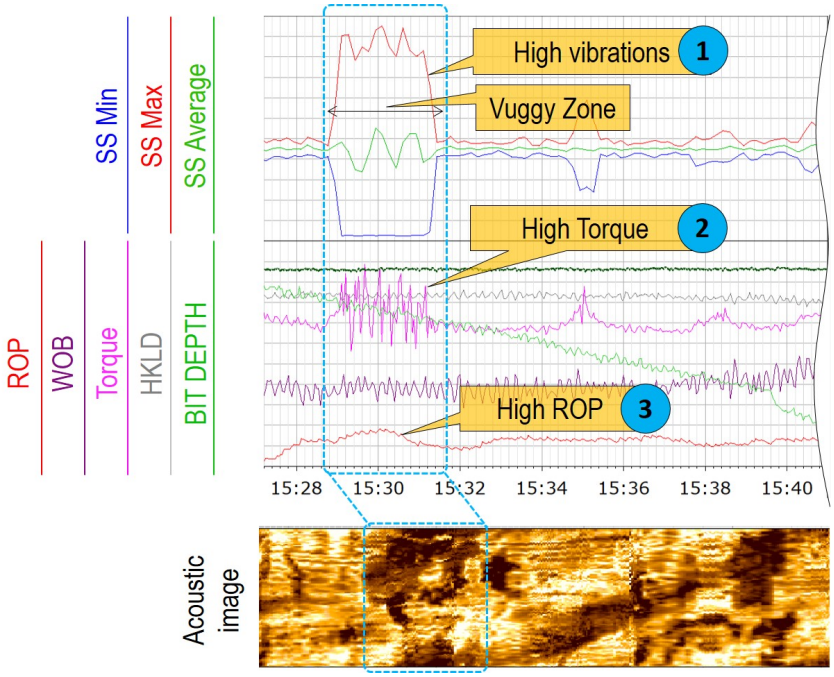

Figure 7. Drilling mechanics data in the interval of fracture and vugs (Well #2).

The third example illustrates drilling (Well #3) through a 6 m vuggy interval of cm-scale vugs framed by two erosive surfaces as shown in Figure 8. The length of the interval helps us to assess drillstring dynamics in the extended vugs zone, without any other geological features crossed by the well path, as can be seen in the borehole image. These conductive patches are interpreted as large vugs, which are probably formed due to post-depositional (e.g., karstic) carbonate dissolution. The beginning of drilling in this interval is characterized by a drilling break. As pointed out in Figure 8, entering the vuggy zone is accompanied by high ROP (arrow #2) and sharp drop of WOB (arrow #3). Drilling within the vuggy interval is accompanied by a constant high level of shocks displayed on the top track in the figure and colored in green, red and blue curves. The interval of higher levels of shocks in comparison with the outer intervals is marked with arrow #1. This example confirms that a high level of S&V may be associated with an interval of karstification.

This section has reviewed the key aspects of drillstring behavior in zones of karstification. A high level of shocks, ROP increase, drill breaks within carbonate intervals can often indicate that the well path is going through a karstification object and may be close to other karsts. However, these indicators have drawbacks. As will be shown in the next section, drillstring dynamics is often not sensitive enough to detect some small-scale features or filled caves, which are also important signs of karstification zones and indicators of intervals with a high likelihood of karsts. In the section that follows, we will consider a set of additional indicators, which can significantly improve the detection of karsts and small-scale geological features that can be missed by drilling dynamics measured by surface and downhole sensors.

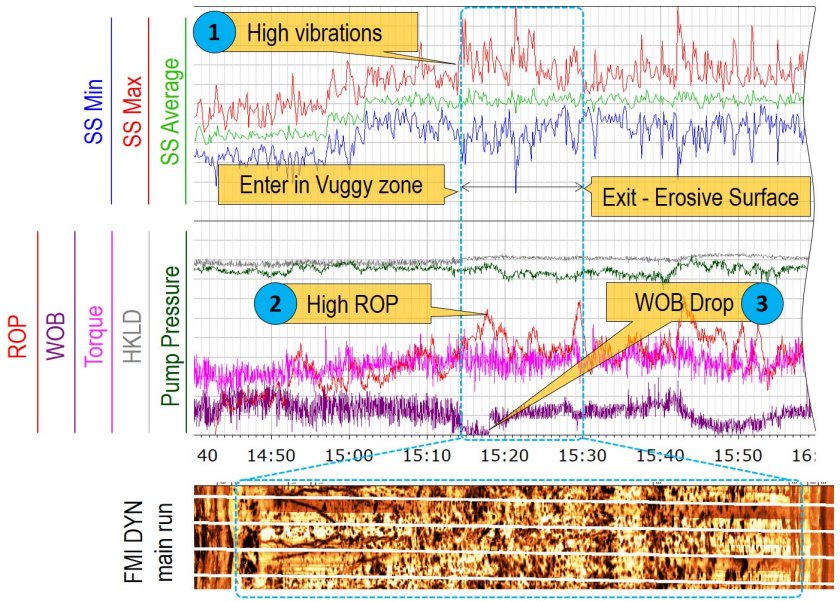

Figure 8. Drilling mechanics data in the 6 m (19.7 ft)interval of vugs 6 m thickness (Well #3).

4. Detection of Karsts Based on Flow-Data

So far, we have focused on the drilling dynamics data. In this section, we will consider a set of flow-based indicators of karsts. This will enable us to consider the problem of karst detection based on a fundamentally different set of measurements, which might significantly increase the accuracy of the detection of karstification objects. In this section, we will identify patterns corresponding to karsts based on flow measurements.

Drilling mud is essential for many drilling tasks, from cuttings transfer to transmitting hydraulic energy to downhole tools. Drilling mud is pumped through main rig pumps to the Kelly hose, it enters the drill collars, sprays out of the drilling nozzles and is pushed up in the annulus to the surface mud cleaning system and is then pumped back again. Analysis of the difference between inflow and outflow rates (delta-flow) underlies kick/loss monitoring and reservoir characterization methods. The range of applications of this methodology is linked to the accuracy of delta-flow measurements. Delta-flow analysis presented in this section is based on precise measurements of the inflow and outflow using flowmeters integrated in a Controlled Mud Level (CML) system [31], which was utilized in drilling in the region of our study.

The benefit of the flow-based approach for advance karst detection is based on a different type of measurements. In contrast to drillstring dynamics analysis, the flow-based approach allows one to determine not only open caves (e.g., by specific BHA behavior in the intervals of karstification: drill-break etc.), but also caves filled with clastic material. For instance, in the case of a filled cave, depending on the mechanism of cave genesis and the clastic material property, there may be no clearly detectable changes in ROP that can be linked to drilling through this karstification object.

Figure 9 represents the time plot of drilling Well #4 where a combination of two different types of measurements are available. The first and second tracks (from top to bottom) marked on the figure as "standard drilling data" display the same set of measurements as discussed earlier in Wells 2 and 3. A set of additional measurements marked in the figure as "CML Data" is shown in the upper track. The lowest track displays the borehole image with marked intervals of vugs and cavity. Interval 1 in the figure represents the response of drilling-based and flow-based measurements in the cm to dm scale interval of vugs. This interval begins with a drilling break, represented by a drop of WOB (arrow #1) with simultaneous increase of ROP (arrow #2). After that the ROP profile, the level of shocks as well as other drilling parameters remain constant in this interval. It proves the limitation of

the drilling dynamics approach, as it is not accurate enough to detect small changes in the rock properties.

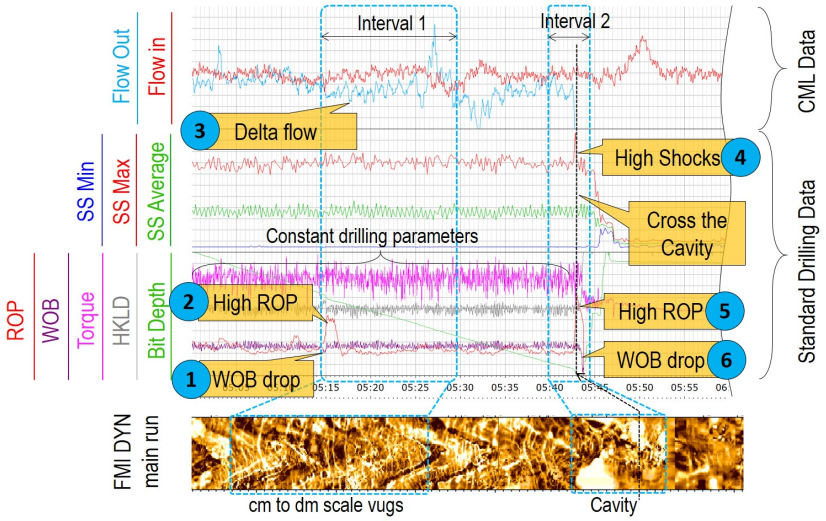

Figure 9. Drilling through the intervals of vugs and cave. Standard and flow data (Well #4).

However, an analysis of the CML data can reveal some additional information. When the bit passes through a zone with vugs or fractures, drilling mud invades some of the open channels, which results in a consequent drop in the riser level (arrow #3). The initial point, when the first difference between the inflow and outflow is noticed correlates with the interval of the vugs facies defined by the borehole image.

Interval 2 illustrates an example of drilling through a cave. The initial depth of the cave boundary is defined by the borehole image and represents the beginning of interval 2. As can be noted, at the depth defined by the borehole image there are no visible changes in any measurements. However, in close proximity to the cave there are spiky changes in the mud losses. Mud losses in the interval of the cave reached 2000 L/min (528.3 gal (US)/min). The clear response can be noticed by a step change of many logged parameters, such as S&V (arrow #4), ROP (arrow #5), WOB (arrow #6).

The next example demonstrates the response of the drillstring dynamics and delta-flow during drilling through bedding planes and Drilling Induced Fractures (Well #5). For convenience, the track order and drilling measurements are displayed similarly to the previous example. As can be seen in Figure 10, for all three intervals the S&V level remains constant (arrows #1, #2 and #3). The ROP profile at the beginning of each interval (marked with arrows #4, #5 and #6) has similar behavior to the ROP in the karstified interval from the previous example: increased drilling speed can be seen when the drill bit enters the interval. However, the profile of the mud losses is different across these intervals and, for example, in the interval of DIF, there is a delta immediate recovery of the outflow, which indicates the initiation of DIF and subsequent filling with the drilling mud (arrow #7).

In this section, we have discussed the applicability of flow-based measurements for karst detection. The examples demonstrate that drilling dynamics-based and flow-based indicators can complement each other in detecting karstification objects. A delta-flow profile might reveal additional signs of karstification in the intervals that are undetectable through drilling mechanics measurements, such as filled caves or small vugs. Detection of even small forms of karstification can be an important part of early karst detection methodology, as they can indicate drilling in a karstified zone. The studied intervals of vugs are characterized by moderate values of fluid losses (delta flow), without significant fluctuations, in contrast to cave intervals demonstrating a step change in the delta-flow profile.

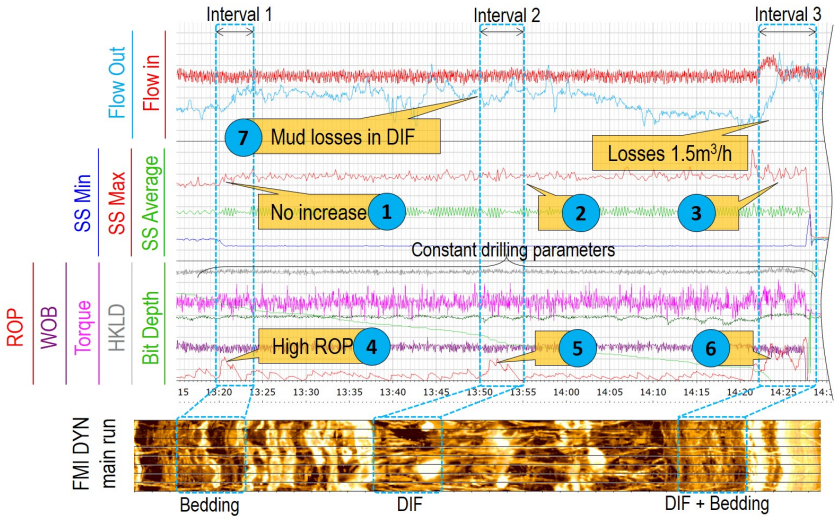

Figure 10. Drilling in the intervals of bedding and drilling induced fractures. Standard and flow data (Well #5).

5. Results and Discussion

In this paper, we have studied the problem of encountering karsts while drilling. We have analyzed 20 wells drilled in karstified carbonates in the Barents Sea region and completed a detailed study of the corresponding data: drilling events and end-of-well reports, borehole image and core sample data, recorded time-domain data of BHA dynamics and mud flow data. Based on this analysis we have concluded that karsts are often preceded by various karstification objects that form karstification zones.

These objects generate specific patterns in drilling data. When monitored and detected, these patterns can be utilized as indicators of karstification zones with a high likelihood of encountering karsts. The availability of such indicators can support decision-making processes to improve drilling safety. The list of the identified patterns corresponding to various karstification objects is presented in Table 1.

Table 1. Patterns of drilling measurements/events corresponding to karstification objects.

Karst Type	Drilling Break	ROP	S & V	Torque	Mud Losses
Cavities	Often when entering	Step change	Highest lateral vibrations	Highest variations	Step change in mud loss profile
Vugs	Not always detected, size-dependable	Higher ROP while in vugs	Higher compared to other intervals	No/small variations	Constant moderate loss profile
Fractures	Typically no	Increase/ Not always detected	Small/ No increase	No/small variations	Decrease and immediate recovering profile

This work is the first step towards developing tools for detecting karstification zones and mitigating risks related to drilling in karstified formations. Still, with the limited amount of wells available for this study (wells that are located in one geographical area), the presented results should be utilized in the context of all available information and experience.

This study is limited in terms of specific geology and the number of wells available for the analysis. Even in carefully studied fields, the percentage of wells that encountered

karsts and at the same time had a full set of necessary well-log data (e.g., borehole images, or accurate delta-flow data) is rather small. Moreover, some of the intervals have to be additionally excluded from the analysis of drilling/mud flow response in karsts: only intervals with constant drilling/pump/mud parameters should be kept in order to evaluate the unique patterns of drilling measurements corresponding to karsts and not other possible factors affecting drilling.

Future work on this subject should be directed towards obtaining and analyzing well data from more wells, including wells from fields with different geology. This will allow one to create a more complete and statistically reliable picture of real-time indicators of karsts and karstification zones, regardless of the geography of the research region. Such an analysis can be performed utilizing the same workflow developed and employed in this paper.

Another direction for further work is to develop algorithms for the automatic detection of karst patterns in the drilling data, e.g., algorithms based on machine learning principles. A karst encountered during drilling can be considered an anomaly in the drilled formation. One can employ various machine learning methods to automatically detect these anomalies from the real-time drilling data. When the karst patterns in the drilling data presented in this paper are confirmed with data from a sufficiently large number of wells, one can employ them in pattern recognition algorithms [47–51] for the automatic detection of karsts from the drilling data. Additionally, one should apply various filters to the drilling data to enable accurate and timely detection of karsts by advanced algorithms [52–54]. As indicated in one of the recent studies [55], nonlinear filters can be efficient for the automated detection of instances when a drilling measurement signal experiences a fast and noticeable change in the trend, such as when encountering karsts.

With more data available, one can also work on establishing sets of logic-based rules to detect and identify specific karstification objects and karstification intervals with higher confidence, avoiding or reducing the challenges of false-positive and false-negative detection. The development of such algorithms for the automatic real-time detection of karstification objects and zones from available drilling data is a direction for further research and development.

Author Contributions: Conceptualization, D.M. and S.S.; Formal analysis, D.M.; Investigation, D.M.; Methodology, D.M., A.P. and S.S.; Resources, A.P. and S.S.; Software, D.M. and A.P.; Supervision, A.P. and S.S.; Validation, D.M. and A.P.; Writing—review & editing, D.M., A.P. and S.S. All authors have read and agreed to the published version of the manuscript, please turn to the CRediT taxonomy (http://img.mdpi.org/data/contributor-role-instruction.pdf) for the term explanation.

Funding: This research was funded by Lundin Energy.

Institutional Review Board Statement: Not applicable.

Informed Consent Statement: Not applicable.

Data Availability Statement: Data sharing not applicable.

Acknowledgments: This research is a part of BRU21—NTNU Research and Innovation Program in Digital and Automation Solutions for the Oil and Gas Industry (www.ntnu.edu/bru21) (accessed on 5 May 2022) and supported by Lundin Energy Norway AS. In particular, we wish to thank Per Haugum, Bård Fjellså and Andy Clark from Lundin Norway AS, for their decisive technical contributions in important stages of this research. In addition, special thanks are given to Eric Claudey from Enhanced Drilling for his valuable support on the CML part of this paper. The authors would like to thank Mai Britt Mørk from NTNU, for providing expert advice and support on the geological study of the problem. Stewart Clark is acknowledged for editing the language in the final version of the paper.

Conflicts of Interest: The authors declare that they have no known competing financial interest or personal relationships that could have appeared to influence the work reported in this paper.

Abbreviations

The following abbreviations are used in this manuscript: (For readers unfamiliar with the technology used in the oil and gas industry, we refer to a review of definitions given in https://glossary.oilfield.slb.com/, accessed on 5 May 2022).

BHA	Bottom Hole Assembly
CML	Controlled Mud Level
CPI	Computer Processed Interpretation
DIF	Drilling Induced Fractures
LCM	Lost Circulation Material
LWD	Logging While Drilling
MPD	Managed Pressure Drilling
MWD	Measurements While Drilling
PMCD	Pressurized Mud Cap Drilling
RCD	Rotational Controll Device
ROP	Rate Of Penetration
SPP	Stand Pipe Pressure
S&V	Shocks and Vibrations
UCS	Uniaxial Compressive Strength
WL	Wireline Logging
WOB	Weight On Bit

References

1. Joshi, R.; Singh, K.H. Carbonate Reservoirs: Recent Large to Giant Carbonate Discoveries Around the World and How They Are Shaping the Carbonate Reservoir Landscape. In *Carbonate Reservoirs: Recent Large to Giant Carbonate Discoveries Around the World and How They Are Shaping the Carbonate Reservoir Landscape*; Springer: Singapore, 2020; Chapter 2, pp. 3–14. [CrossRef]
2. Gawor, L.; Jonczy, I. Surface Karst Landforms of the Notranjska region (south-western Slovenia). *Geotourism/Geoturystyka* **2014**, *37*, 55–60. [CrossRef]
3. Nas, S.W. Deepwater Managed Pressure Drilling Applications. In Proceedings of the SPE International Oil and Gas Conference and Exhibition in China, Beijing, China, 8–10 June 2010; pp. 1–9. [CrossRef]
4. Ziegler, R.; Ashley, P.; Malt, R.F.; Stave, R.; Toftevåg, K.R. Successful Application of Deepwater Dual Gradient Drilling. In Proceedings of the SPE/IADC Managed Pressure Drilling and Underbalanced Operations Conference and Exhibition, San Antonio, TX, USA, 12–13 April 2013.
5. Ghalambor, A.; Salehi, S.; Shahri, M.P.; Karimi, M. Integrated Workflow for Lost Circulation Prediction. In Proceedings of the SPE International Conference and Exhibition on Formation Damage Control, Lafayette, LA, USA, 27 February 2014. [CrossRef]
6. Reitsma, D. A simplified and highly effective method to identify influx and losses during Managed Pressure Drilling without the use of a Coriolis flow meter. In Proceedings of the SPE/IADC Managed Pressure Drilling and Underbalanced Operations Conference and Exhibition, Kuala Lumpur, Malaysia, 24–25 February 2010. [CrossRef]
7. Alshubbar, G.D.; Nygaard, R. Curing Losses in Vuggy Carbonate Formations. In Proceedings of the SPE/IADC Middle East Drilling Technology Conference and Exhibition, Abu Dhabi, UAE, 29–31 January 2018. [CrossRef]
8. Savari, S.; Whitfill, D.L. Managing Lost Circulation in Highly Fractured, Vugular Formations: Engineering the LCM Design and Application. In Proceedings of the Abu Dhabi International Petroleum Exhibition and Conference, Abu Dhabi, United Arab Emirates, 11–14 November 2019. [CrossRef]
9. Muir, K. MPD techniques address problems in drilling Southeast Asia's fractured carbonate structures. In *International Association of Drilling Contractors*; Drilling Contractor: Galveston, TX, USA, 2006; pp. 34–36.
10. Goodwin, B.; Nauduri, S.; Medley, G. MudCap Drilling: New Variations, Drivers, Limitations, and Lessons Learned—Case Histories. In Proceedings of the SPE/IADC Managed Pressure Drilling and Underbalanced Operations Conference and Exhibition, Madrid, Spain, 8–9 April 2014; pp. 1–7. [CrossRef]
11. Houng, N.H.; Gallo Zapata, J.F.; Ahmad Fauzi, M.A. PMCD Technique Enables Coring & Wireline Logging Operations in Total Lost Circulation. In Proceedings of the SPE/IADC Drilling Conference and Exhibition, Fort Worth, TX, USA, 1–3 March 2016; pp. 1–13. [CrossRef]
12. Jayah, M.N.; A Aziz, I.A.; Mathews, T.; Voshall, A.; Rojas Rodriguez, F. Implementation of PMCD to Explore Carbonate Reservoirs from SemiSubmersible Rigs in Malaysia results in Safe and Economical Drilling Operations. In Proceedings of the SPE/IADC Drilling Conference and Exhibition, Amsterdam, The Netherlands, 5–7 March 2013; pp. 1–15. [CrossRef]
13. Kyi, K.K.; Han, M.; Lee, S.; Roberts, I.; Maeso, C. Maximising Logging While Drilling Value in Carbonate Wells Drilled in Pressurised Mud Cap Drilling Conditions: Challenges, Solutions, and Advances. In Proceedings of the SPE Asia Pacific Oil and Gas Conference and Exhibition, Nusa Dua, Indonesia, 20–22 October 2015; pp. 1–12. [CrossRef]
14. Amanbayev, Y.; Karmanov, K. Successful Implementation of PMCD Technology in Kazakhstan. In Proceedings of the SPE Russian Petroleum Technology Conference, Moscow, Russia, 15–17 October 2018; pp. 1–10. [CrossRef]

15. Godhavn, J.M.; Hauge, E.; Molde, D.O.; Kjøsnes, I.; Gaassand, S.; Fossli, S.B.; Stave, R. ECD Management Toolbox for Floating Drilling Units. In Proceedings of the OTC Offshore Technology Conference, Houston, TX, USA, 5–8 May 2014; pp. 1–23. [CrossRef]
16. Li, S.; Wen, S.; Gao, Y.; Zhao, J.; Feng, X. High Resolution 3D Seismic for Mapping Of Subsurface Karsting of Carbonate. In Proceedings of the World Petroleum Congress (WPC), Rio de Janeiro, Brazil, 1–5 September 2002; pp. 90–99.
17. Peiling, M.; Dong, L.; Yonglei, L.; Haiting, A.; Xingyin, X.; Qiang, X.; Zujun, W.; Xiangzhou, Z. Seismic Reflection Characteristics of Deeply-Buried, Layered, Karstic Carbonate Reservoir Strata. In Proceedings of the SEG International Exposition and Annual Meeting, Houston, TX, USA, 22–27 September 2013; pp. 1–6. [CrossRef]
18. Sheriff, R. Factors affecting seismic amplitude. *Geophys. Prospect.* **1975**, *23*, 125–138. [CrossRef]
19. Wang, N.; Xie, X.B.; Duan, M.C.; Li, D.; Wu, R.S. Improving seismic image resolution in a carbonate fracture cave region: A case study. In *SEG Technical Program Expanded Abstracts 2019*; Society of Exploration Geophysicists: Houston, TX, USA, 2019; Chapter 1, pp. 32–36. [CrossRef]
20. Claudey, E.; Fossli, B.; Elahifar, B.; Qiang, Z.; Olsen, M.; Mo, J. Experience Using Managed Pressure Cementing Techniques with Riserless Mud Recovery and Controlled Mud Level in the Barents Sea. In Proceedings of the SPE Norway Subsurface Conference, Bergen, Norway, 18 April 2018; pp. 1–18. [CrossRef]
21. Maia, W.; Rubio, R.; Junior, F.; Haldorsen, J.; Guerra, R.; Dominguez, C. First Borehole Acoustic Reflection Survey mapping a deepwater turbidite sand. In Proceedings of the 2006 SEG Annual Meeting, New Orleans, LA, USA, 1–6 October 2006; Volume 25, pp. 87–92. [CrossRef]
22. Kim, J.H.; Schon, J.; Towle, G.; Whitman, W.W. An Automatic Inversion Of Normal Resistivity Logs. *Petrophysics* **1990**, *31*, 1–10.
23. Wu, P.T.; Lovell, J.R.; Clark, B.; Bonner, S.D.; Tabanou, J.R. Dielectric-Independent 2-MHz Propagation Resistivities. In Proceedings of the SPE Annual Technical Conference and Exhibition, Houston, TX, USA, 3–6 October 1999. [CrossRef]
24. Yang, H.J.; Guo, S.S.; Gao, Y.D.; Chen, M.; Wang, C.; Shim, Y.H.; Chang, B.T.; Wang, F.; Li, T. Reduce Drilling Risk in HPHT Gas Field Using Innovative Look-Ahead Technology—A Case Study from South China Sea. In Proceedings of the IPTC International Petroleum Technology Conference, Dhahran, Kingdom of Saudi Arabia, 13–15 January 2020. [CrossRef]
25. Laouafa, F.; Guo, J.; Quintard, M. Underground Rock Dissolution and Geomechanical Issues. *Rock Mech. Rock Eng.* **2021**, *54*, 3423–3445. [CrossRef]
26. Bella, P. Genetic Types of Caves in Slovakia. *Acta Carsologica* **1998**, *27*, 15–23. [CrossRef]
27. Palmer, A. Origin and morphology of limestone caves. *Geol. Soc. Am. Bull.* **1991**, *103*, 1–21. [CrossRef]
28. Waltham, A.; Fookes, P. Engineering classification of karst ground conditions. *Q. J. Eng. Geol. Hydrogeol.* **2003**, *36*, 101–118. [CrossRef]
29. Peng, C.; Dai, J.; Yang, S. Seismic Guided Drilling: Near Real Time 3D Updating of Subsurface Images and Pore Pressure Model. In Proceedings of the IPTC International Petroleum Technology Conference, Beijing, China, 26–28 March 2013; pp. 1–6. [CrossRef]
30. Terwogt, J.; Makiaho, L.; van Beelen, N.; Gedge, B.; Jenkins, J. Pressured Mud Cap Drilling from A Semi-Submersible Drilling Rig. In Proceedings of the SPE/IADC Drilling Conference, London, UK, 17–19 March 2015; Society of Petroleum Engineers: Amsterdam, The Netherlands, 2005; pp. 1–6. [CrossRef]
31. Bysveen, J.; Fossli, B.; Stenshorne, P.C.; Skargord, G.; Hollman, L. Planning of an MPD and Controlled Mud Cap Drilling CMCD Operation in the Barents Sea Using the CML Technology. In Proceedings of the SPE/IADC Managed Pressure Drilling and Underbalanced Operations Conference and Exhibition, Rio de Janeiro, Brazil, 28–29 March 2017. [CrossRef]
32. Tangen, G.I.; Smaaskjaer, G.; Bergseth, E.; Clark, A.; Fossli, B.; Claudey, E.; Qiang, Z. Experience from Drilling a Horizontal Well in a Naturally Fractured and Karstified Carbonate Reservoir in the Barents Sea Using a CML MPD System. In Proceedings of the SPE/IADC Managed Pressure Drilling and Underbalanced Operations Conference and Exhibition, Amsterdam, The Netherlands, 9–10 April 2019; pp. 1–19. [CrossRef]
33. Niznik, M.R.; Elks, W.C.; Zeilinger, S.C. Pressurized Mud Cap Drilling in Qatar's North Field. In Proceedings of the IADC/SPE Managed Pressure Drilling and Underbalanced Operations Conference & Exhibition, San Antonio, TX, USA, 12–13 February 2009; Society of Petroleum Engineers: San Antonio, TX, USA, 2009; pp. 1–11. [CrossRef]
34. Maksimov, D.; Pavlov, A.; Sangesl, S. Drilling in Karstified Carbonates: Early Risk Detection Technique, Volume 11: Petroleum Technology. In Proceedings of the International Conference on Offshore Mechanics and Arctic Engineering, Online, 3–7 August 2020. [CrossRef]
35. Collins, T. Analysis of Torsional Shock during Drilling. In Proceedings of the SPE/IADC Drilling Conference, Amsterdam, The Netherlands, 5–7 March 2013; Society of Petroleum Engineers: Amsterdam, The Netherlands, 2013; pp. 1–7.
36. Balka, M.S.; Ghazzawi, A.; Melgares, H. A Novel Approach for Mitigation of Shocks & Vibration and Achieving Drilling Performance in Carbonate Reservoirs. In *SPE Kingdom of Saudi Arabia Annual Technical Symposium and Exhibition*; Society of Petroleum Engineers: Dammam, Saudi Arabia, 2018; pp. 1–8. [CrossRef]
37. Dhelie, P.E.; Danielsen, V.; Lie, J.E.; Evensen, A.K.; Wright, A.; Salaun, N.; Rivault, J.L.; Siliqi, R.; Grubb, C.; Vinje, V.; et al. Improving seismic imaging in the Barents Sea by source-over-cable acquisition. In *SEG Technical Program Expanded Abstracts 2018*; SEG: Houston, TX, USA, 2018; Chapter 2, pp. 71–75. [CrossRef]
38. Macpherson, J.; Mason, J.; Kingman, J. Surface Measurement and Analysis of Drillstring Vibrations While Drilling. In Proceedings of the SPE/IADC Drilling Conference and Exhibition, Amsterdam, The Netherlands, 23–25 February 1993. [CrossRef]

39. Kirkman, M. Use of Surface Measurement of Drillstring Vibrations to Improve Drilling Performance. In Proceedings of the World Petroleum Congress (WPC), Stavanger, Norway, 29 May 1994.
40. Wylie, R.; Soukup, I.; Mata, H.; Cuff, S.; Ho, A. The Drilling Optimization Benefits of Direct Drillstring Surface Measurements—Case Studies from Field Operations. In Proceedings of the SPE/IADC Drilling Conference and Exhibition, London, UK, 17–19 March 2015; Society of Petroleum Engineers: London, UK, 2015; pp. 1–28. [CrossRef]
41. Tanguy, D.; Zoeller, W. Applications Of Measurements While Drilling. In Proceedings of the SPE Annual Technical Conference and Exhibition, San Antonio, TX, USA, 5–7 October 1981; pp. 1–16. [CrossRef]
42. Grosso, D.S.; Raynal, J.C.; Rader, D. Report on MWD Experimental Downhole Sensors. *J. Pet. Technol.* **1983**, *35*, 899–904. [CrossRef]
43. LeGros, F.W., Jr.; Martin, C. Applications of Measurements While Drilling (MWD): Development of the East Breaks Field, Offshore Texas. In Proceedings of the SPE/IADC Drilling Conference and Exhibition, New Orleans, LA, USA, 6–8 March 1985; pp. 1–9. [CrossRef]
44. Warren, T.; Oster, J.; Sinor, L.; Chen, D. Shock Sub Performance Tests. In Proceedings of the SPE/IADC Drilling Conference and Exhibition, Dallas, TX, USA, 3–6 March 1998; pp. 1–13. [CrossRef]
45. Teale, R. The concept of specific energy in rock drilling. *Int. J. Rock Mech. Min. Sci. Geomech. Abstr.* **1965**, *2*, 57–73. [CrossRef]
46. Onyia, E. Relationships Between Formation Strength, Drilling Strength, and Electric Log Properties. In Proceedings of the SPE Annual Technical Conference and Exhibition, Houston, TX, USA, 2–5 October 1988; pp. 1–14. [CrossRef]
47. Fair, M.L.; Campbell, S.L.Active incipient fault detection in continuous time systems with multiple simultaneous faults. *Numer. Algebr. Control. Optim.* **2011**, *1*, 211. [CrossRef]
48. Auxiliary signals for improving fault detection. In *Auxiliary Signal Design in Fault Detection and Diagnosis*; Zhang, X.J., Ed.; Springer: Berlin/Heidelberg, Germany, 1989; pp. 45–91. [CrossRef]
49. Scott, J.K.; Marseglia, G.R.; Magni, L.; Braatz, R.D.; Raimondo, D.M. A hybrid stochastic-deterministic input design method for active fault diagnosis. In Proceedings of the 52nd IEEE Conference on Decision and Control, Firenze, Italy, 10–13 December 2013. [CrossRef]
50. Scott, J.R.; Campbell, S. Auxiliary signal design for failure detection in differential-algebraic equations. *Numer. Algebr. Control. Optim.* **2014**, *4*, 151. [CrossRef]
51. Nikoukhah, R. Guaranteed Active Failure Detection and Isolation for Linear Dynamical Systems. *Automatica* **1998**, *34*, 1345–1358. [CrossRef]
52. Gui, M.W. The Basics of Noise Detection and Filtering for Borehole Drilling Data. *Open Civ. Eng. J.* **2008**, *2*, 1–10. [CrossRef]
53. Babu, C.N.; Reddy, B.E. A moving-average filter based hybrid ARIMA–ANN model for forecasting time series data. *Appl. Soft Comput.* **2014**, *23*, 27–38. [CrossRef]
54. Voigtman, E.; Winefordner, J.D. Low-pass filters for signal averaging. *Rev. Sci. Instrum.* **1986**, *57*, 957–966. [CrossRef]
55. Maksimov, D.; Løken, M.A.; Pavlov, A.; Sangesl, S. Automated Pattern Recognition in Real-Time Drilling Data for Early Karst Detection. In Proceedings of the International Conference on Offshore Mechanics and Arctic Engineering, Hamburg, Germany, 5–10 June 2021. [CrossRef]